NLO Properties of Metallabenzene-Based Chromophores: A Time-Dependent Density Functional Study

Amir Karton, Mark A. Iron, Milko E. van der Boom,* and Jan M. L. Martin*

Department of Organic Chemistry, Weizmann Institute of Science, 76100 Rehovot, Israel

Received: December 12, 2004; In Final Form: March 1, 2005

The static and dynamic first hyperpolarizabilities for a series of substituted metallabenzene-based nonlinear optical (NLO) chromophores were determined by time-dependent density functional theory (TDDFT). The electronic excitation contributions to the first hyperpolarizability are rationalized in terms of the two-level model. The effects on the hyperpolarizabilities of (a) the metal center (Os, Ir, Pt); (b) the ligand environment (PH_3, CO, Cl); (c) various donor and acceptor substituents (NH_2, OH, Me, H, Cl, Br, I, COOMe, COOH, CN, NO_2); and (d) the length of π-conjugation were studied. Our calculations predict that metallabenzenes have significant second-order NLO susceptibilities, ranging from $\beta_{tot}^0 = 1.0 \times 10^{-29}$ to 5.6×10^{-28} esu and from $\mu\beta_{tot}^0 = 3.0 \times 10^{-47}$ to 1.1×10^{-44} esu, that can be tuned by changing the metal center and/or ligand environment.

Introduction

Ever since Marder and co-workers demonstrated in 1987 that ferrocene derivatives have large second harmonic generation (SHG) efficiencies,[1] numerous experimental and theoretical studies have been devoted to the understanding of the structure−property relationships and the optimization of second-order optical properties of metal-based chromophores.[2−27] Two classes of complexes that were extensively studied are metallocenes,[1,7−21] where the π-ligand is strongly coupled to the metal, and pyridine-based complexes,[3,22−27] where there is relatively weak coupling to the metal center. Nevertheless, the design of conceptually new high-β-complexes remains an interesting and challenging task.

Metallabenzenes form an intriguing class of organometallic complexes where the metal is part of an aromatic π-system (Scheme 1).[28−39] Two of the six π-electrons are metal d-electrons delocalized over the π-system and, therefore, are expected to be far more polarizable than the d-electrons of other organometallic complexes. Several metallabenzene complexes have been isolated,[29] including osmabenzenes,[30,31] iridabenzenes[32−34] and platinabenzenes.[35] We recently reported a series of computational studies on the reactivity and stability of these complexes.[36−39] The reduced aromaticity of metallabenzenes[36,40] relative to benzene and heteroaromatic rings, as indicated, for example, by their absolute hardness[41] values (i.e., 2.27, 2.17, and 0.60 eV for benzene, thiophene, and $(3,5\text{-}Me_2C_5H_3Ir)(PEt_3)_3$, respectively),[42] is also expected to play an important role in the nonlinear optical (NLO) properties of these complexes. The replacement of phenyl rings in traditional organic donor−π-bridge−acceptor (D−π−A) chromophores with aromatic heteroaromatic rings, such as thiophene or thiazole, has been shown, both experimentally[43−47] and theoretically,[48−50] to significantly enhance hyperpolarizabilities. This increase in hyperpolarizability was rationalized by (i) the lower aromatic delocalization energy of the heteroaromatics relative to benzene, which lowers the energy gap between the ground state and the charge transfer (CT) excited state,[51] (ii) inductive effects of the electron-rich or electron-poor ring on the donor or the acceptor, respectively, and (iii) increased electron density of the π-bridge.

SCHEME 1: Resonance Forms of Metallabenzenes

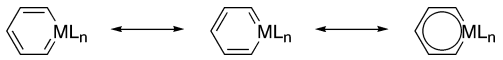

Organic NLO materials have potential applications in areas such as electrooptics and photonics.[52−55] NLO materials interact with electromagnetic fields to produce new electromagnetic fields altered in frequency and phase. These effects arise from nonlinear polarization of the molecule. At the microscopic level, they are governed by the third-rank tensor $\boldsymbol{\beta}$, which corresponds to the third-order term of the Taylor expansion of the energy with respect to an electric field. Assuming that only one excited state is coupled strongly enough to the ground state by the applied electric field to contribute to $\boldsymbol{\beta}$, and that only one tensor component (β_{xxx}) dominates the NLO response (i.e., a one-dimensional CT transition), then the second-order nonlinearity ($\boldsymbol{\beta}$) can be approximated by the two-level model[56,57]

$$|\boldsymbol{\beta}| \approx \beta_{xxx} = \beta_{xxx}^0 R(\omega) = \frac{3e^2 \Delta\mu_{ge} f_{ge}}{2(\hbar\omega_{ge})} \frac{\omega_{ge}^4}{(\omega_{ge}^2 - \omega^2)(\omega_{ge}^2 - 4\omega^2)} \quad (1)$$

where β_{xxx}^0 is the static hyperpolarizability component along the CT axis, $R(\omega)$ is the resonance enhancement factor, ω_{ge} is the transition energy to the lowest CT excited state, f_{ge} is the corresponding oscillator strength, $\Delta\mu_{ge} = \mu_e - \mu_g$ is the difference in the dipole moments between the excited and ground states, and ω is the excitation energy. This model has been shown to be reliable for many organic systems, such as para-substituted benzenes,[47] 4,4′-disubstituted stilbenes,[47] and 4,4′-disubstituted diphenylacetylenes,[58] but fails for many organometallic systems for which generally more than one transition dominates the NLO properties.[14,27] One exception is the Ru(II)-4,4′-bipyridinium class of complexes that has a metal-to-ligand charge transfer (MLCT) excitation in the visible region

* Corresponding authors. E-mail: milko.vanderboom@weizmann.ac.il; comartin@wicc.weizmann.ac.il.

10.1021/jp0443456 CCC: $30.25 © 2005 American Chemical Society
Published on Web 05/28/2005

SCHEME 2: Metallabenzene Derivatives[a]

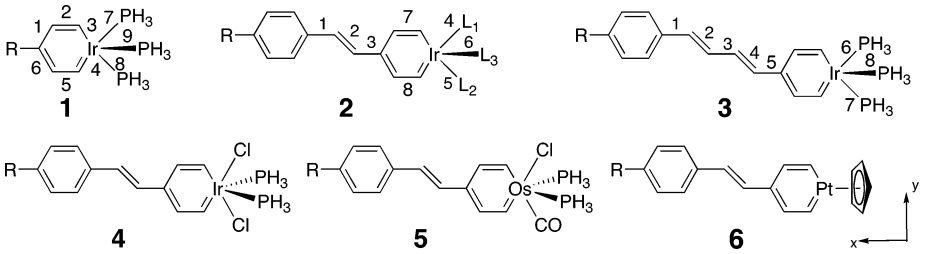

[a] L_1, L_2 = PH_3, CO, $H_2P(CH_2)_2PH_2$; L_3 = PH_3, CO; R = NH_2, OH, Me, H, Cl, Br, I, COOMe, COOH, CN, NO_2, C(CN)=C(CN)$_2$, NH_3^+. The bond numbering scheme for compounds **1**−**3** used throughout the paper is shown.

that accounts for a large portion of the hyperpolarizability.[59,60] The two-level model gives a simple interpretation to the sign of the static hyperpolarizability (β^0_{xxx}), that is, it has the same sign as $\Delta\mu_{ge}$. The two-level model predicts that $\boldsymbol{\beta}$ becomes exceptionally high at $\omega \approx \omega_{ge}$ and $\omega \approx \omega_{ge}/2$. Therefore, when comparing the molecular second-order NLO responses of different chromophores, $\boldsymbol{\beta}^0$ should be considered in order to eliminate resonance enhancements and to afford qualitative insights.

Computational chemistry can afford insights into structure−property relationships of molecules and has been demonstrated to be of particular value in the rational design of NLO chromophores.[7,21,61−66] Computational methods have been used to calculate the responses of otherwise inaccessible structural variations, such as the effect of biphenyl dihedral angle rotation.[61] Several series of organic[62−65] and organometallic[7,21,66] NLO chromophores with remarkable NLO responses have been identified by computational chemistry.

We report here on a systematic computational investigation of the NLO properties of several analogues of experimentally prepared metallabenzenes using time-dependent density functional theory (TDDFT). TDDFT is becoming an increasingly powerful tool in recent years for the investigation of high-order electronic response properties of organometallic complexes,[67−70] especially because of the rapid increase in available computer power and the recent development of linear scaling techniques.[71,72] The main goal here is to evaluate the use of metallabenzene moieties for the design of molecular NLO chromophores and to obtain insight into the structure−function relationships of these systems. It was found that metallabenzenes have significant second-order NLO susceptibilities that can be tuned widely by changing the metal center and/or ligand environment.

Computational Details

Geometry optimizations were carried out using *Gaussian 98* revision A.11[73] and *Gaussian 03* revision C.01.[74] The B97-1[75] DFT hybrid exchange correlation functional was used in conjunction with the SDD basis set-relativistic effective core potential (RECP) combination. B97-1, which was locally implemented into a modified revision of *Gaussian 98*, has been shown to be more accurate for equilibrium properties than other DFT functionals.[76] SDD includes the Huzinaga−Dunning double-ζ basis set on the lighter elements with the Stuttgart−Dresden basis set−RECP combination[77] on the transition metals. Equilibrium geometries were verified to have all real harmonic frequencies.

The linear and nonlinear optical property calculations were performed using the response module[78,79] of the Amsterdam Density Functional (ADF) version 2003.01[71,80,81] program suite. Scalar relativistic effects were included using the zero-order regular approximation (ZORA) formalism.[82−84] For the response calculations, the statistical average of orbital potential (SAOP)[85] exchange-correlation functional was used. This functional corrects the asymptotic region of the Kohn−Sham potential and has been shown to yield more accurate excitation energies and frequency-dependent hyperpolarizabilities than LDA or other GGA functionals.[85,86]

It is well-known that electronic response properties, such as $\boldsymbol{\beta}$, require a description of the regions of space far from the nuclei; that is, the asymptotic behavior of the basis functions is of key importance when calculating high-order electronic response properties (see, for example, refs 87−89). We used a double-augmented double-ζ (dADZ) Slater-type basis set, which is still computationally affordable for the organometallic complexes studied. The two sets of added diffuse functions were obtained according to the basis set completeness profile procedure of Chong.[90] Both sets of diffuse functions are given in Table S1 of the Supporting Information.

Results and Discussion

The ground-state dipole moments (μ), the quadratic static and frequency dependent molecular hyperpolarizabilities along the dipole moment direction (β^0_{vec} and β^{1064}_{vec}), and the total intrinsic hyperpolarizabilities (β^0_{tot} and β^{1064}_{tot}) were calculated for a series of metallabenzenes **1**−**6** (Scheme 2), concentrating on the stilbene-like metallabenzenes **2**, **4**, **5**, and **6**.

The conjugated organic fragments of metallabenzenes **1**, **4**, **5**, and **6** are essentially planar. In compounds **2** and **3**, there is a small twist of ∼6−8° around single bonds 3 and 5, respectively. Compounds **1**, **2**, **3**, and **6** belong to the C_1 point group, while compounds **4** and **5** have C_S symmetry. The equatorial ligands of compounds **1**−**3** are bent slightly out of the molecular plane by approximately 10° and the apical ligand points up by about 80°. Table 1 lists the B97-1/SDD optimized bond lengths of compound **1** with various R-groups along with their Hammett constants (σ_p).[91] Bonds 1, 3, 4, and 6 are lengthened, while bonds 2 and 5 are shortened, as the donating or accepting strength of the R-group increases (see Scheme 2 for definition of bond numbering). These changes in the bond lengths indicate a larger contribution of the zwitterionic (non-aromatic) quinonoid resonance structure to the ground state of these derivatives as the accepting or donating strength of the R-group increases (Scheme 3).

Table 2 lists the B97-1/SDD optimized bond lengths of bonds 1−6 for compound **2** with three phosphine ligands and various R-groups (Scheme 2). Single bonds 1 and 3 are shortened, while double bond 2 is lengthened, as the donating or accepting strength of the R-group is increased (e.g., when going from H to NH_2 and C(CN)═C(CN)$_2$, the single bond 1 is shortened by 0.004 Å and 0.016 Å, respectively, and the double bond 2 is lengthened by 0.001 Å and 0.008 Å, respectively). It is,

TABLE 1: B97-1/SDD Optimized Bond Lengths (Å) of Compound 1 with Various R-Groups[a]

		bond								
R	σ_p[b]	1	2	3	4	5	6	7	8	9
NH_2	−0.57	1.427	1.399	1.990	1.990	1.399	1.427	2.434	2.434	2.384
OH	−0.38	1.415	1.401	1.993	1.982	1.407	1.414	2.442	2.441	2.374
H	0.00	1.414	1.409	1.987	1.987	1.409	1.414	2.447	2.447	2.356
Cl	0.24	1.406	1.409	1.985	1.985	1.409	1.406	2.448	2.448	2.361
COOH	0.44	1.419	1.404	1.987	1.989	1.402	1.421	2.454	2.454	2.341
CN	0.70	1.422	1.404	1.986	1.986	1.404	1.422	2.453	2.454	2.348
NO_2	0.81	1.415	1.402	1.989	1.989	1.402	1.415	2.458	2.458	2.338

[a] See Scheme 2 for definition of bond numbering. [b] From ref 91.

SCHEME 3: Limiting Resonance Forms of Compounds 1 and 2, Where R Represents an Acceptor[a]

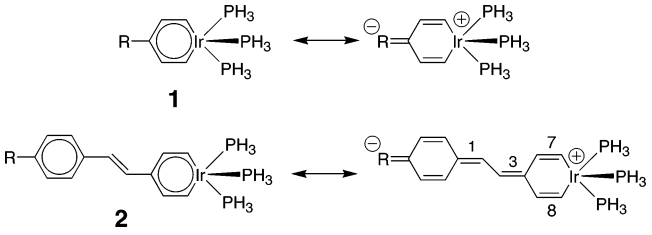

[a] Left: aromatic structure. Right: zwitterionic, non-aromatic quinonoid structure. For donors, the zwitterionic form has the opposite charge separation.

TABLE 2: B97-1/SDD Optimized Bond Lengths (Å) of Compound 2 with L_1, L_2, and L_3 = PH_3 and Various R-Groups[a]

		bond					
R	σ_p[b]	1	2	3	4	5	6
NH_2	−0.57	1.470	1.369	1.470	2.444	2.445	2.361
OH	−0.38	1.473	1.368	1.470	2.446	2.447	2.358
Me	−0.14	1.474	1.368	1.470	2.446	2.447	2.358
H	0.00	1.474	1.368	1.470	2.447	2.448	2.357
Cl	0.24	1.473	1.368	1.470	2.448	2.449	2.356
Br	0.26	1.473	1.368	1.470	2.448	2.449	2.356
I	0.28	1.473	1.368	1.469	2.448	2.449	2.356
COOMe	0.44	1.470	1.370	1.468	2.449	2.450	2.354
CN	0.70	1.469	1.370	1.467	2.450	2.451	2.353
NO_2	0.81	1.465	1.372	1.465	2.452	2.453	2.350
$C(CN)=C(CN)_2$	N/A[c]	1.458	1.376	1.460	2.455	2.455	2.345
NH_3^+	0.6	1.455	1.380	1.454	2.462	2.463	2.338

[a] See Scheme 2 for definition of bond numbering. [b] From ref 91. [c] Not available.

therefore, evident that only the strongest acceptors, such as $C(CN)=C(CN)_2$, NH_3^+, and to a lesser extent NO_2, induce some double-bond character in single bonds 1 and 3 and single-bond character in double bond 2. Although the maximum variation in bond length does not exceed 0.02 Å, it indicates a larger contribution of the zwitterionic resonance structure to the ground state of these acceptor derivatives (Scheme 3), resulting in a lower degree of bond-length alternation[8,92] and hence a more polarized π-system. The ring bond lengths (Supporting Information, Table S2) also support this observation. The same trends are clearly observed also for compound **3** (Supporting Information, Table S3).

The Ir−PH_3 bond lengths of compound **2** listed in Table 2 also follow a general trend. The bond lengths of the two equatorial phosphines (bonds 4 and 5) increase, while the bond length of the apical phosphine (bond 6) decreases, with higher accepting strength (σ_p)[91] of the R-group. These general trends are also observed for compounds **1** (Table 1) and **3** (Supporting Information, Table S3).

Table 3 collates linear and nonlinear optical properties for chromophore **2** with three phosphine ligands and various

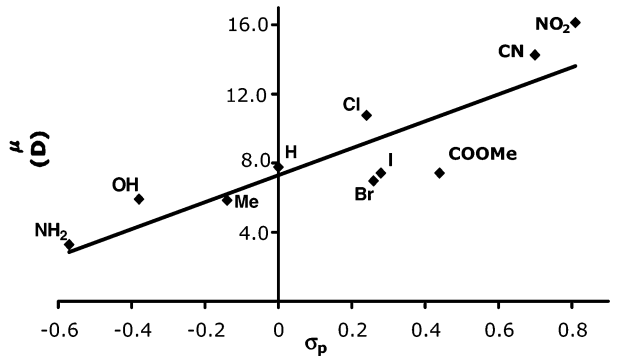

Figure 1. Dipole moment (μ) versus σ_p Hammett constants (σ_p) for the iridastilbenes **2** (L_1, L_2, L_3 = PH_3) in Table 3 (except for tricyanovinyl for which no σ_p value is available and NH_3^+ that induces a very large dipole moment of 24 D not reflected by its σ_p value of 0.6). The line has a linear correlation coefficient of $R^2 = 0.75$.

R-groups. The dipole moment component along the CT axis (μ_x) is the only component that substantially changes from one R-group to another. For all the metallabenzenes in Table 3, the metal center behaves as a donor in the ground state, as demonstrated by the negative μ_x for all the neutral derivatives and by the general increase of μ_x with the accepting strength of the R-group (Figure 1). This is not surprising, since the C_5H_4-$Ir(PH_3)_3$ moiety is electron-rich.[32]

The negative sign of β^0_{vec} for the derivatives R = NH_2, Br, I, OH, and Me (Table 3) can be explained on the basis of the $Ir(PH_3)_3$ fragment acting as an electron donor in the ground state and an electron acceptor in the $\boldsymbol{\beta}$-determining excited state because of a ligand-to-metal charge transfer (LMCT) excitation in the opposite direction to the dipole moment. The net result is a reduction of the dipole moment in the excited state, and hence, a negative β^0_{vec} value according to the two-level model (see eq 1). For the derivatives in which R = Cl, H, COOMe, CN, NO_2, and $C(CN)=C(CN)_2$ (Table 3), the $\boldsymbol{\beta}$-determining MLCT excitation enhances the dipole moment resulting in positive β^0_{vec} values. The negative β^0_{vec} for NH_3^+ is a result of the reduction of the dipole moment upon MLCT excitation. Thus, neutral R-groups with a negative β^0_{vec} can be regarded as donors, and those with a positive β^0_{vec} as acceptors, in the $\boldsymbol{\beta}$-determining excited state. Note, however, that according to this definition Br and I would be donors even though they are acceptors according to their positive Hammett constants (σ_p).[91]

For the iridastilbenes **2** listed in Tables 3 and 4, the static hyperpolarizability component along the ground-state dipole moment (β^0_{vec}) is very close, in absolute value, to the static total intrinsic first hyperpolarizabilities (β^0_{tot}). Thus, the CT excitation is essentially unidirectional and parallel to the ground-state dipole moment. The COOMe, CN, NO_2, $C(CN)=C(CN)_2$, and NH_3^+ derivatives in Table 3 and the additional complexes listed in Table 4 are also characterized by one dominant hyperpolarizability component (β^0_{xxx}) that lies along the CT

TABLE 3: Linear and Nonlinear Optical Properties of Compound 2 (L_1, L_2, L_3 = PH_3; Scheme 2) with Various R-Groups[a]

R	σ_p[b]	μ	μ_x	β^0_{vec}	β^0_{tot}	β^{1064}_{vec}	β^{1064}_{tot}	$\mu\beta^0_{tot}$	λ_1	f_1
NH_2	−0.57	3.29	−2.07	−51.5	76.3	−570.7	875.1	251.0	576	0.327
Br	0.26	6.96	−6.50	−35.8	37.0	−609.2	645.1	257.5	588	0.320
I	0.28	7.42	−6.99	−28.4	29.0	−825.6	867.5	215.2	588	0.361
OH	−0.38	5.92	−5.40	−28.0	29.5	−470.9	511.8	174.6	587	0.282
Me	−0.14	5.86	−5.26	−9.6	9.6	−411.9	449.5	56.3	590	0.275
Cl	0.24	10.76	−10.44	7.6	9.2	−407.9	415.5	99.0	596	0.284
H	0.00	7.76	−7.34	30.2	32.9	−314.1	325.2	255.3	590	0.286
COOMe	0.44	7.41	−6.48	86.2	98.9	−596.5	647.0	732.8	628	0.373
CN	0.70	14.26	−14.01	116.3	118.8	−572.9	579.7	1694.1	641	0.392
NO_2	0.81	16.13	−15.90	307.2	312.1	−1070.2	1084.3	5034.2	817	0.316
C(CN)=C(CN)$_2$	N/A[c]	18.84	−18.60	522.9	530.4	−11098.8	11179.1	9992.7	895	0.428
NH_3^+	0.6	24.32	24.20	−133.9	134.5	146.8	147.4	3271.0	704	0.366

[a] β in units of 10^{-30} esu, $\mu\beta$ in units of 10^{-48} esu, μ in D (=10^{-18} esu), and λ_1 in nm. [b] σ_p from ref 91. [c] Not available.

TABLE 4: Linear and Nonlinear Optical Properties for Compound 2 (Scheme 2) with Various Ligands (L_1, L_2, L_3 = PH_3, CO, $H_2P(CH_2)_2PH_2$) and R-Groups (R = NO_2 and NH_2)[a]

R	L_1	L_2	L_3	μ	μ_x	β^0_{vec}	β^0_{tot}	β^{1064}_{vec}	β^{1064}_{tot}	$\mu\beta^0_{\tau o\tau}$	λ_1	f_1
NO_2	$H_2P(CH_2)_2$	PH_2	PH_3	18.23	−18.11	328.5	329.9	−1316.8	1320.4	6014.1	867	0.289
NO_2	PH_3	PH_3	PH_3	16.13	−15.90	307.2	312.1	−1070.2	1084.3	5034.2	817	0.316
NO_2	CO	PH_3	PH_3	13.33	−11.98	268.2	300.7	−879.6	995.6	4008.3	832	0.284
NO_2	CO	CO	PH_3	10.28	−8.14	221.3	282.5	−747.0	911.6	2904.1	786	0.303
NO_2	CO	CO	CO	3.20	−3.19	112.7	113.3	−1485.1	1492.8	362.6	611	0.374
NH_2	PH_3	PH_3	PH_3	3.29	−2.07	−51.5	76.3	−570.7	875.1	251.0	576	0.327
NH_2	PH_3	PH_3	CO	2.98	−1.24	−42.4	92.9	−381.6	903.2	276.8	491	0.941
NH_2	CO	PH_3	PH_3	6.26	3.24	52.9	114.3	276.9	461.8	715.5	562	0.560
NH_2	CO	CO	PH_3	9.32	7.00	69.5	97.1	453.1	582.2	905.0	540	0.552
NH_2	CO	CO	CO	10.75	10.74	116.9	117.0	−14300	14326	1277.2	534	0.995

[a] β in units of 10^{-30} esu, $\mu\beta$ in units of 10^{-48} esu, μ in D (=10^{-18} esu), and λ_1 in nm.

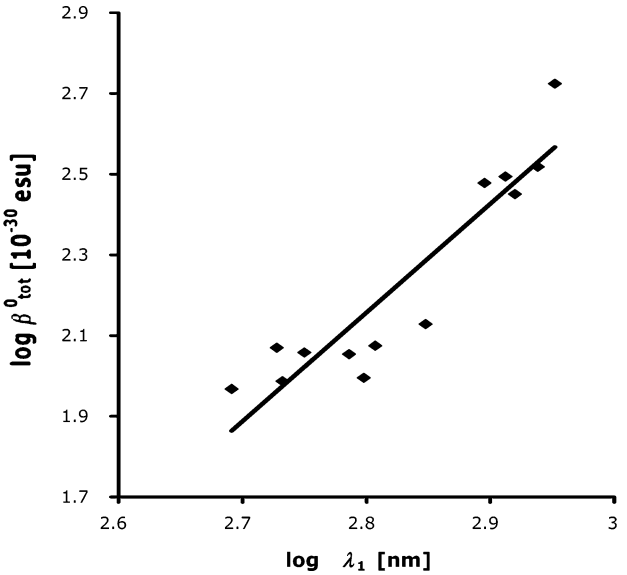

Figure 2. Logarithmic plot of the static first hyperpolarizability (β^0_{tot}) versus the wavelength of the lowest transition energy (λ_1) for the iridabenzenes **2** in Tables 3 and 4 (excluding the trisphosphine, NH_2, Br, I, OH, Me, Cl, and H derivatives; see text). The solid line has a linear correlation coefficient of $R^2 = 0.85$.

direction and is at least one order of magnitude larger than the other components of $\boldsymbol{\beta}$. The two-level model[56,57] establishes a connection between the first hyperpolarizability and a low-lying one-dimensional CT transition (eq 1). The validity of this approximation for the iridastilbenes **2** in Tables 3 and 4 is illustrated by the logarithmic correlation between β^0_{tot} and the wavelength of the lowest-energy transition λ_1 (Figure 2). Only the complexes that have only one dominant hyperpolarizability component (β^0_{xxx}) are considered (vide supra). The correlation coefficient $R^2 = 0.85$ suggests that the first transition plays an important role in determining $\boldsymbol{\beta}$ and that the $\Delta\mu_{ge} f_{ge}$ product (see eq 1) remains relatively constant for this class of complexes and does not significantly dictate trends in β^0_{tot}. Note that the oscillator strengths remain relatively constant for all the complexes considered except for the last four R = NH_2 derivatives in Table 4. In fact, if we exclude these four donor derivatives from the logarithmic plot (the four points on the left in Figure 2), then the correlation coefficient (R^2) becomes 0.94.

The first electronic transition is primarily composed of the HOMO → LUMO transition (0.82−0.87 for complex **2** with L_1, L_2, L_3 = PH_3, Table 3). The HOMO and LUMO of complex **2** (L_1, L_2, L_3 = PH_3, Table 3) with R = NH_2, H, and NO_2 are shown in Figure 3 (those for the rest of the R groups are shown in the Supporting Information, Figure S1). The HOMO for all the complexes in Table 3 is largely localized on the metal center and is very similar to the typical aromatic metallabenzene HOMO.[36] The LUMO for all but the very strong acceptors (NH_3^+, NO_2, and C(CN)=C(CN)$_2$), apart from having metal contributions, is largely localized on double bonds 1, 3, 7, and 8 (Scheme 3, right structure); that is, it corresponds to the nonaromatic zwitterionic resonance structure. As the accepting strength of the R-group increases, the LUMO, which has $3d_{z^2}$ metal contributions, gradually moves from the metallabenzene ring (when R = H) to the R-substituted ring. Moreover, the LUMO is mainly acceptor-based for the strongest acceptors (NO_2 and C(CN)=C(CN)$_2$). These HOMO and LUMO orbitals indicate an increase in the degree of MLCT upon HOMO → LUMO transition with an increase in the accepting ability of the R-group. As a consequence, β^0_{vec} also increases with an increase in the accepting strength of the R-group. For the NH_2, Br, I, OH, and Me derivatives, the negative sign of β^0_{vec} indicates, as discussed, a $\boldsymbol{\beta}$-determining LMCT excitation. For these derivatives, the LUMO composition is not sensitive to the nature of the R-group. Furthermore, there is a reduction in

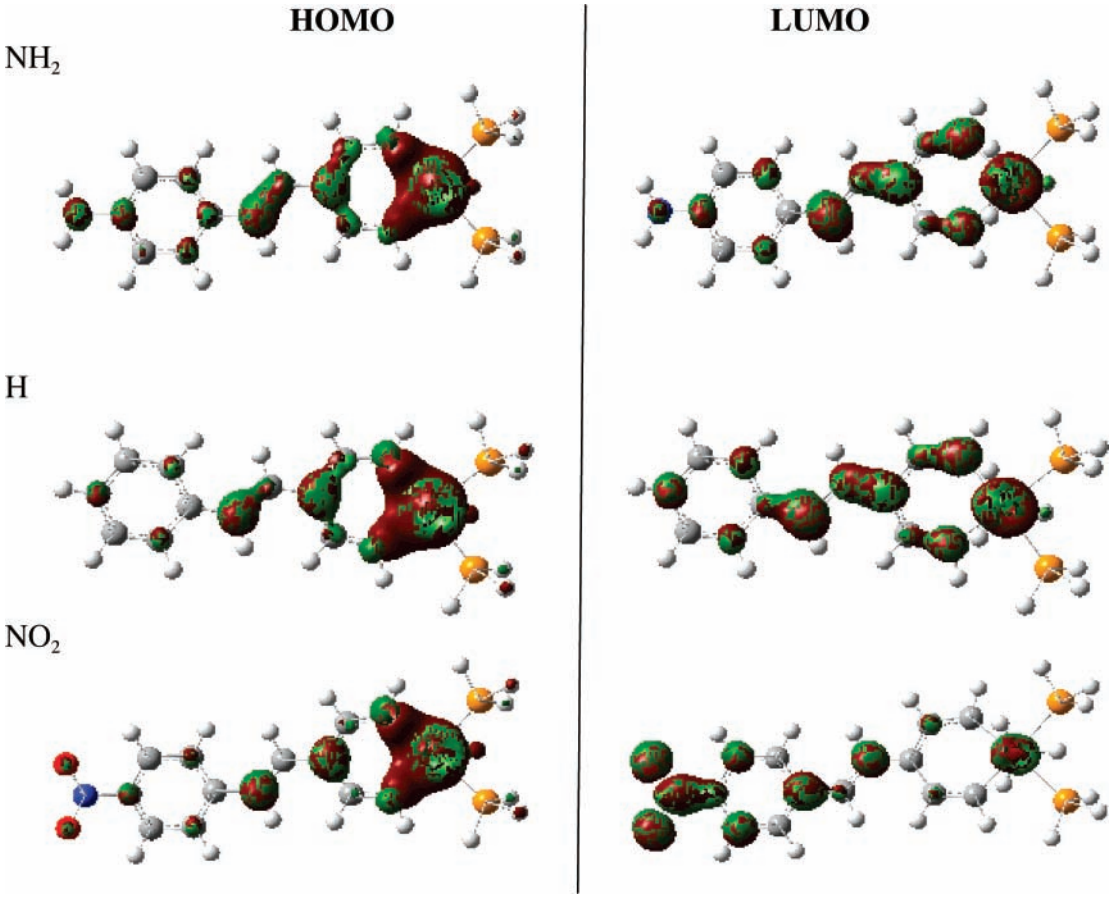

Figure 3. HOMO and LUMO of the iridastilbenes **2** (L_1, L_2, L_3 = PH_3; R = NH_2, H, NO_2), calculated at the B97-1/SDD level of theory. Atomic color scheme: H, white; C, gray; N, blue; O, red; P, orange; Ir, indigo.

the electron density on the metal center upon HOMO → LUMO excitation. Therefore, it is not likely that the HOMO → LUMO transition has a large contribution to the second-order responses of these derivatives.

The energies of the first transition (λ_1) for the acceptor derivatives listed in Table 3 are strongly affected by the accepting strength of the R-group (e.g., λ_1 is 590, 628, 641, and 817 nm for H, COOMe, CN, and NO_2, respectively). This red-shift parallels the increase in static first hyperpolarizabilities (i.e., β^0_{tot} is 30.2 × 10^{-30}, 86.2 × 10^{-30}, 116.3 × 10^{-30}, and 307.2 × 10^{-30} esu, respectively). For the donor derivatives, however, λ_1 is only slightly affected by the R-group (e.g., λ_1 is 576, 588, 587, and 590 nm for NH_2, Br, OH, and Me, respectively). Moreover, these shifts are not consistent with the β^0_{tot} values, which decrease (not increase!!) as λ_1 is red-shifted (i.e., β^0_{tot} is 73.6 × 10^{-30}, 37.0 × 10^{-30}, 29.5 × 10^{-30}, and 9.6 × 10^{-30} esu, respectively). This suggests either that the first transition is not the ***β***-determining transition or that more than one transition governs the NLO responses of these derivatives. The lowest transition that is, in general, blue-shifted when going from strong to weak donors is the third electronic transition (i.e., λ_3 = 474 nm for NH_2, 468 nm for I, 457 nm for Br, 447 nm for OH, and 439 nm for Me with oscillator strengths of 0.395, 0.340, 0.360, 0.284, and 0.288, respectively). λ_3 is primarily composed of the HOMO-2 → LUMO transition, which is also the second largest contributor to λ_1. However, a logarithmic plot between λ_3 and β^0_{tot} for the donor derivatives gives a low correlation coefficient (R^2 = 0.71).

For compound **2** with three phosphine ligands and acceptor R-groups (Table 3), β^0_{vec} is positive and increases in the order

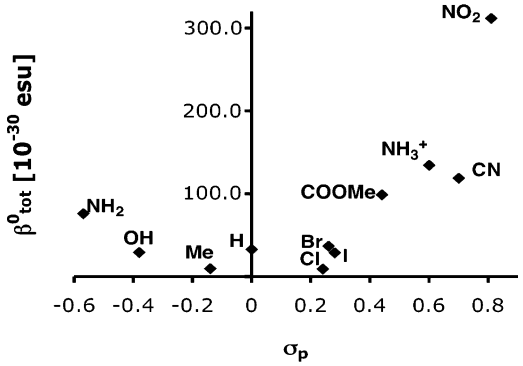

Figure 4. Plot of static hyperpolarizability (β^0_{tot}) versus the σ_p Hammett constants (from ref 91) for the iridabenzenes **2** in Table 3 (except tricyanovinyl for which no σ_p value is available).

H < COOMe < CN < NO_2 < C(CN)═C(CN)$_2$ in accordance with the electron-accepting strength of the R-group. On the other hand, with donor R-groups, β^0_{vec} is negative and decreases in the order Me > OH > I > Br > NH_2. Coupled with the directions of the ***β***-determining charge transfer transitions (i.e., MLCT for R = acceptor and LMCT for R = donor), this suggests that the iridium center can behave as either a donor or an acceptor in the ***β***-determining excited state depending on the R-substituent. As a result, both strong donors and acceptors have high hyperpolarizabilities (Figure 4). This amphoteric donor−acceptor role of the metal center has been previously observed for other organometallic complexes, including pentacarbonyltungsten(0) stilbazole derivatives,[27] chromium(0) carbonyl arene complexes,[15] and rhodium(I), iridium(I), and osmium(II) pyridine carbonyl complexes.[25]

TABLE 5: NLO Properties of Trisphosphine Complexes 1, 2, and 3 (Scheme 2) for Various R-Groups (NH_2, Br, OH, H, CN, and NO_2)[a]

R	compound	μ	μ_x	β^0_{vec}	β^0_{tot}	β^{1064}_{vec}	β^{1064}_{tot}	$\mu\beta^0_{tot}$
NH_2	**1**	2.19	−1.22	−9.9	13.0	−23.2	23.6	28.5
	2	3.29	−2.07	−51.5	76.3	−570.7	875.1	251.0
Br	**1**	6.4	−5.94	−16.5	17.1	−33.29	33.5	109.4
	2	6.96	−6.50	−35.8	29.5	−609.2	645.1	205.3
OH	**1**	5.34	−4.64	−10.9	11.7	−17.5	19.3	62.5
	2	5.92	−5.40	−28.0	29.5	−470.9	511.8	174.6
	3	5.87	−4.58	−33.9	40.5	−1777.7	2206.8	237.7
H	**1**	5.26	−4.65	−7.7	7.8	−10.7	14.5	41.0
	2	7.76	−7.34	30.2	32.9	−314.1	325.2	255.3
CN	**1**	11.94	−11.69	−5.0	5.1	−105.0	113.1	60.9
	2	14.26	−14.01	116.3	118.8	−572.9	579.7	1694.1
NO_2	**1**	13.58	−13.35	5.1	5.6	−45.8	46.5	76.0
	2	16.13	−15.90	307.2	312.1	−1070.2	1084.3	5034.2
	3	18.69	−18.43	555.1	563.5	−4587.7	4618.6	10531.8

[a] β in units of 10^{-30} esu, $\mu\beta$ in units of 10^{-48} esu, and μ in D ($=10^{-18}$ esu).

The dynamic hyperpolarizabilities β^{1064}_{tot} of **2** also show this amphoteric donor−acceptor behavior, and both the stronger donors and acceptors have larger dynamic hyperpolarizabilities than the weaker ones (e.g., $\beta^{1064}_{tot} = 1084.3 \times 10^{-30}$ esu for NO_2, 325.2×10^{-30} esu for H, and 875.1×10^{-30} esu for NH_2). The frequency-dependent hyperpolarizabilities β^{1064}_{vec} are all negative. A physical explanation based on the two-level model is that the resonance enhancement factor $R(\omega)$ (eq 1) is positive for the donor derivatives (i.e., $\lambda_{ge} < 532$ nm or $\lambda_{ge} > 1064$ nm) and negative for the acceptor derivatives (i.e., 1064 nm $> \lambda_{ge} >$ 532 nm). These requirements are fulfilled by λ_1 for the acceptor derivatives and by λ_3 for the donor derivatives.

Exchanging the phosphine ligands on the iridium center of **2** with carbonyls (Table 4) reduces the electron density on the metal through π-back-bonding and is expected to reduce the push−pull character when R is an acceptor group (NO_2). This is demonstrated by the reduced dipole moments and static hyperpolarizability values as more phosphine ligands are replaced (Table 4). As expected, replacement of the equatorial phosphines (L_1 and L_2) by the more electron-rich $H_2P(CH_2)_2$-PH_2 fragment enhances the dipole moment and hyperpolarizability values. The first electronic transition is blue-shifted as the metal center becomes more electron-poor, consistent with the decrease in the β^0_{vec} values. When the R-substituent is a strong donor (NH_2) and the ligand environment is composed of three phosphine ligands, β^0_{vec} is negative. Again, this indicates a reduction of the dipole moment in the ***β***-determining excited state caused by an LMCT excitation. Replacing the apical phosphine with a carbonyl group reduces the absolute values of the dipole moment along the CT direction (μ_x) and β^0_{vec}. Replacing the phosphine in the L_1 position, however, inverts the dipole moment direction and also the sign of β^0_{vec}. The positive sign of β^0_{vec} indicates an enhancement of the dipole in the ***β***-determining excited state caused by an LMCT excitation. Further replacement of phosphines with carbonyls increases both μ_x and β^0_{vec}. These results demonstrate that the first hyperpolarizability can be significantly tuned by changing the ligands (L_1, L_2, L_3) on the iridium center, a common feature of many organometallic chromophores.[2,3] Again for the R = NH_2 derivatives (Table 4), there is no correlation between β^0_{tot} and λ_1, indicating that the first electronic transition might not be ***β***-determining or that more than one transition governs the NLO responses of these derivatives. It is interesting to note, however, that for the tris-carbonyl complex, for which the wavelength of the first transition ($\lambda_1 = 534$ nm) is nearly equal to one-half the wavelength at which the hyperpolarizabilities were determined (1064 nm), the dynamic hyperpolarizabilities are anomalously high, indicating a dramatic resonance enhancement.

TABLE 6: NLO Properties of Compounds 4, 5, and 6 (Scheme 2) for Various R-Groups (NH_2, OH, H, COOH, and NO_2)[a]

R	μ	μ_x	β^0_{vec}	β^0_{tot}	β^{1064}_{vec}	β^{1064}_{tot}	$\mu\beta^0_{tot}$
				Compound **4**			
NH_2	16.82	16.77	102.8	102.9	2198.7	2199.9	1730.8
OH	12.02	12.01	74.1	74.3	641.9	644.8	893.6
H	10.21	10.01	31.3	31.4	280.6	280.7	320.5
COOH	9.19	9.18	19.0	19.0	310.8	311.3	174.2
NO_2	3.63	3.63	−46.5	47.0	−87.4	98.1	170.7
				Compound **5**			
NH_2	12.96	12.84	115.1	116.9	2677.6	2708.4	1515.0
OH	9.55	9.50	72.2	78.1	555.5	598.2	745.9
H	6.70	5.66	17.4	19.5	−0.1	65.8	130.7
COOH	5.42	5.41	6.1	6.6	191.7	198.6	35.8
NO_2[b]	3.32	−2.41	142.0	196.0	−2373.7	4013.9	650.7
				Compound **6**			
NH_2[b]	8.02	8.01	127.5	127.7	−2083.0	2086.7	1024.2
OH	4.88	4.48	85.1	92.2	3771.0	4082.7	449.9
H	3.27	3.25	39.4	39.6	432.2	434.3	129.5
COOH	3.72	3.41	44.2	49.0	1269.9	1400.0	182.3
NO_2	3.66	−3.54	60.8	62.2	−5554.2	5711.6	227.4

[a] β in units of 10^{-30} esu, $\mu\beta$ in units of 10^{-48} esu, and μ in D ($=10^{-18}$ esu). [b] These values should be taken with caution due to a suspiciously large extra DFT term related to g_{xc}.[78]

It is well-known that an increase in the π-conjugation length can significantly enhance the quadratic hyperpolarizabilities of organic[46,47,93−95] and organometallic[2] chromophores. Increasing the conjugation length substantially enhances the static and dynamic second-order NLO responses (Table 5). For instance, when going from compound **1** to **2**, β^0_{tot} is enhanced by factors of 5.8, 4.2, and 56.1, while the enhancement factors for β^{1064}_{tot} are 37.1, 22.4, and 23.3 for R = NH_2, H, and NO_2, respectively. For comparison, an enhancement by a factor of ∼4 in β^{1910}_{tot} is measured experimentally when going from *para*-aminonitrobenzene to 4,4′-aminonitrostilbene.[47] When going from compound **2** to compound **3**, β^0_{tot} is enhanced by factors of 1.4 and 1.8, while β^{1064}_{tot} by factors of 3.8 and 4.3, for OH and NO_2, respectively. Slightly lower enhancements are obtained for related organic (∼1.4)[96] and organometallic (∼2)[15,97] chromophores.

Similar to most of the derivatives of compound **2**, compounds **4**, **5**, and **6** (Table 6) are also characterized by $|\beta^0_{vec}| \approx \beta^0_{tot}$ and by one dominant hyperpolarizability component that lies parallel

to the CT axis. When the metal center is in a higher oxidation state (compounds **4**, **5**, and **6**), it is more electron-withdrawing. Thus, the metal centers of compounds **4**, **5**, and **6** are expected to induce larger electronic asymmetry along the CT axis with donor R-groups, and conversely with acceptor R-groups, compared to compounds **2**. The dipole moment components along the CT axis (μ_x) of compound **2** (L_1, L_2, $L_3 = PH_3$) and compound **4** are antiparallel. Moreover, for compound **2**, it increases, while for compound **4**, it decreases, when going from donors to acceptors. These trends in dipole moments indicate that the $IrCl_2(PH_3)_2$ fragment in **4** behaves as an acceptor in the ground state. The β^0_{vec} values of compound **4** are positive for all but the NO_2 derivative and increase in the order COOH < H < OH < NH_2, suggesting a $\boldsymbol{\beta}$-determining LMCT transition. For the strong acceptor NO_2, however, the negative β^0_{vec} suggests that an MLCT transition dominates $\boldsymbol{\beta}$. Another interesting observation is that a change in the oxidation state of the iridium center can change the nature of the $\boldsymbol{\beta}$-determining transition from an MLCT in compound **2** (with R = H and L_1, L_2, $L_3 = PH_3$) to an LMCT in compound **4** (with R = H).

Replacing the $IrCl_2(PH_3)_2$ fragment (compound **4**) with $OsCl(CO)(PH_3)_2$ (compound **5**) does not change the nature of the $\boldsymbol{\beta}$-determining CT transitions (i.e., MLCT for R = NO_2 and LMCT for the rest). Furthermore, both have similar static and dynamic hyperpolarizabilities when R = NH_2, OH, H, and COOH. However, for the strong acceptor NO_2, compound **5** has a much higher $\boldsymbol{\beta}$-value (e.g., $\beta^0_{tot} = 47.0 \times 10^{-30}$ and 196.0×10^{-30} esu for compounds **4** and **5**, respectively) suggesting that the $OsCl(CO)(PH_3)_2$ fragment is a weaker acceptor. The μ_x values also support this observation: they are consistently lower for compound **5**, and when R = NO_2, μ_x is negative, indicating that for this substituent the $OsCl(CO)(PH_3)_2$ center acts as a donor in the ground state.

The μ_x values of compound **6** indicate that in the ground state the PtCp fragment behaves in a similar manner as the $OsCl(CO)(PH_3)_2$ center of compound **5**, that is, as an acceptor for all R-groups other than NO_2. However, for the Pt chromophore **6**, μ_x is systematically lower than for the Os chromophore **5**, because the more electron-rich PtCp fragment induces less charge asymmetry when R is a donor (NH_2, OH, H, and COOH) and more charge asymmetry when R is an acceptor (NO_2). The nature of the $\boldsymbol{\beta}$-determining CT excitations is the same as for compounds **4**, **5**, and **6** (i.e., MLCT for R = NO_2 and LMCT for the rest). Therefore, it seems that when the metal center is in a relatively high formal oxidation state, the natures of these transitions are metal-independent. The character of low-lying CT excitations for the formally low oxidation state $M(CO)_4L_2$ complexes (M = Cr, Mo, W; L_2 = 2,2′-bipyridine, 1,10-phenanthroline) was also observed experimentally to be metal-independent (i.e., they are all MLCT transitions).[98] These transitions are expected to be the $\boldsymbol{\beta}$-determining MLCT excitations, as was shown experimentally for L_2 = 1,10-phenanthroline.[99]

Conclusions

It is evident from the results given in Tables 1−6 that traditional qualitative arguments for enhancing second-order nonlinear optical responses are applicable for the metallabenzene chromophores **1**−**6** studied.[10,93] Specifically, we have shown that (i) increasing the polarizability (i.e., lowering the bond-length alternation) of the π-bridge results in increased $\boldsymbol{\beta}$ values; (ii) the greater the electronic asymmetry between the donor or acceptor group and the metal fragment, the larger the calculated hyperpolarizability; (iii) the second-order NLO susceptibilities increase as the $\boldsymbol{\beta}$-determining CT transition is bathochromically shifted; and (iv) hyperpolarizability increases with longer π-conjugation. Thus, the metallastilbenes investigated here can be considered counterparts of classical push−pull stilbene chromopores. However, metallastilbenes offer a wide range of metals with different oxidation states and ligand environments and, therefore, have more potential for tunable electronic properties.

It was also found that the electron density of the metallabenzene ring in the first excited state is highly sensitive to the donating/accepting strength of the R-group. We have probed the donor/acceptor nature of Ir, Os, and Pt metallabenzene centers by replacing various substituents distant from the metal center. It is apparent that the metal centers in compounds **1**−**6** can act as both a donor or an acceptor in the $\boldsymbol{\beta}$-determining CT excited state, depending on the R-substituent and ligand environment. However, it seems that, when the metal is in a high oxidation state, the metal identity does not have a substantial effect on the second-order hyperpolarizability.

The calculated second-order hyperpolarizabilities of some of the metallabenzene derivatives are comparable to those of recently reported organometallic chromophores of comparable molecular dimensions. For instance, $[Ru(NH_3)_5$(*N*-(4-acetylphenyl)-4,4′-bipyridinium)(4-(dimethylamino)pyridine)]-$(PF_6)_3$ and *trans*-$[Ru(NH_3)_4$(*N*-(4-acetylphenyl)-4,4′-bipyridinium)]-$(PF_6)_3$[59] were measured to have $\beta^0 = 410 \times 10^{-30}$ and 354×10^{-30} esu, respectively. Compound **2** with three phosphine ligands and R = C(CN)=C(CN)$_2$ is on par with them with $\beta^0 = 530 \times 10^{-30}$ esu. It should be emphasized that, although metallabenzene derivatives are expected to have lower aromatic electron delocalization energies than their organic counterparts (and thus to be less thermodynamically and thermally stable), platinabenzenes, osmabenzenes, and iridabenzenes have been isolated. Therefore, it is concluded that metallabenzenes may be suitable building blocks for the design of novel NLO chromophores.

Acknowledgment. Research was supported by the Helen and Martin Kimmel Center for Molecular Design, the Minerva Foundation (Munich, Germany), the German Federal Ministry for Education and Research (BMBF). J.M.L.M. is the incumbent of the Baroness Thatcher Professorial Chair in Chemistry and a member of the Lise Meitner-Minerva Center for Computational Quantum Chemistry. M.E.vd.B. is the head of the Minerva Junior Research Group (M.J.R.G.) for Molecular Materials and Interface Design, the incumbent of the Dewey David Stone and Harry Levine Career Development Chair, and thanks the Israeli Council of Higher Education for an Alon fellowship. A.K. and M.A.I. acknowledge the Feinberg Graduate School of the Weizmann Institute of Science for M.Sc. and Ph.D. fellowships, respectively. The authors would like to thank Prof. Delano P. Chong (University of British Columbia) for providing a copy of his basis set completeness profile program.

Supporting Information Available: Diffuse functions of the double-augmented double-ζ STO basis set (Table S1), bond lengths and selected dihedral angles of compounds **2** and **3** (Tables S2 and S3), and Cartesian coordinates of all computed geometries. This material is available free of charge via the Internet at http://pubs.acs.org.

References and Notes

(1) Green, M. L. H.; Marder, S. R.; Thompson, M. E.; Bandy, J. A.; Bloor, D.; Kolinsky, P. V.; Jones, R. J. *Nature (London)* **1987**, *330*, 360−362.

(2) Bella, S. D. *Chem. Soc. Rev.* **2001**, *30*, 355−366.
(3) Bozec, H. L.; Renouard, T. *Eur. J. Inorg. Chem.* **2000**, 229−239.
(4) Whittall, I. R.; McDonagh, A. M.; Humphrey, M. G. *Adv. Organomet. Chem.* **1998**, *42*, 291−362.
(5) Long, N. J. *Angew. Chem., Int. Ed. Engl.* **1995**, *34*, 21−34.
(6) Asselberghs, I.; Clays, K.; Persoons, A.; Ward, M. D.; McCleverty, J. *J. Mater. Chem.* **2004**, *14*, 2831−2839.
(7) Calaminici, P. *Chem. Phys. Lett.* **2003**, *374*, 650−655.
(8) Barlow, S.; Henling, L. M.; Day, M. W.; Schaefer, W. P.; Green, J. C.; Hascall, T.; Marder, S. R. *J. Am. Chem. Soc.* **2002**, *124*, 6285−6296.
(9) McDonagh, A. M.; Cifuentes, M. P.; Lucas, N. T.; Humphrey, M. G.; Houbrechts, S.; Persoons, A. *J. Organomet. Chem.* **2000**, *205*, 193−201.
(10) Kanis, D. R.; Ratner, M. A.; Marks, T. J. *Chem. Rev.* **1994**, *94*, 195−242.
(11) Meyer-Friedrichsen, T.; Wong, H.; Prosenc, M. H.; Heck, J. *Eur. J. Inorg. Chem.* **2003**, 936−946.
(12) Zhang, F.; Vill, V.; Heck, J. *Organometallics* **2004**, *23*, 3853−3864.
(13) Lee, I. S.; Choi, D. S.; Dong, M. S.; Chung, Y. K.; Choi, C. H. *Organometallics* **2004,** *23*, 1875−1879.
(14) Barlow, S.; Bunting, H. E.; Ringham, C.; Green, J. C.; Budlitz, G. U.; Boxer, S. G.; Perry, J. W.; Marder, S. R. *J. Am. Chem. Soc.* **1999**, *121*, 3715−3723.
(15) Müller, T. J. J.; Netz, A.; Ansorge, M.; Schmälzlin, E.; Bräuchle, C.; Meerholz, K. *Organometallics* **1999**, *18*, 5066−5074.
(16) Cadierno, V.; Conejero, S.; Gamasa, M. P.; Gimeno, J.; Asselberghs, I.; Houbrechts, S.; Clays, K.; Persoons, A.; Borge, J.; García-Granda, S. *Organometallics* **1999**, *18*, 582−597.
(17) Lee, I. S.; Lee, S. S.; Chung, Y. K.; Kim, D.; Song, N. W. *Inorg. Chim. Acta* **1998**, *279*, 243−248.
(18) Kanis, D. R.; Ratner, M. A.; Marks, T. J. *J. Am. Chem. Soc.* **1992**, *114*, 10338−10357.
(19) Calabrese, J. C.; Cheng, L.-T.; Green, J. C.; Marder, S. R.; Tam, W. *J. Am. Chem. Soc.* **1991**, *113*, 7227−7232.
(20) Matsuzawa, N.; Seto, J.; Dixon, D. A. *J. Phys. Chem.* **1997**, *101*, 9391−9398.
(21) Mang, C.; Wu, K.; Zhang, M.; Hong, T.; Wei, Y. *THEOCHEM* **2004**, *674*, 77−82.
(22) Maury, O.; Viau, L.; Sénéchal, K.; Corre, B.; Guégan, J.-P.; Renouard, T.; Ledoux, I.; Zyss, J.; Bozec, H. L. *Chem.—Eur. J.* **2004**, *10*, 4454−4466.
(23) Dominique, R.; Ugo, R.; Tessore, F.; Lucenti, E.; Quici, S.; Vezza, S.; Fantucci, P.; Invernizzi, I.; Bruni, S.; Ledoux-Rak, I.; Zyss, J. *Organometallics* **2002**, *21*, 161−170.
(24) Coe, B. J.; Harris, J. A.; Brunschwig, B. S. *J. Phys. Chem.* **2002**, *106*, 897−905.
(25) Dominique, R.; Ugo, R.; Bruni, S.; Cariati, E.; Cariati, F.; Fantucci, P.; Invernizzi, I.; Quici, S.; Ledoux, I.; Zyss, J. *Organometallics* **2000**, *19*, 1775−1788.
(26) Briel, O.; Sünkel, K.; Krossing, I.; Nöth, H.; Schmälzlin, E.; Meerholz, K.; Bräuchle, C.; Beck, W. *Eur. J. Inorg. Chem.* **1999**, 483−490.
(27) Kanis, D. R.; Pascal, L. G.; Ratner, M. A.; Marks, T. J. *J. Am. Chem. Soc.* **1994**, *116*, 10089−10102.
(28) Thorn, D. L.; Hoffmann, R. *Nouv. J. Chim.* **1979**, *3*, 39−45.
(29) Bleeke, J. R. *Chem. Rev.* **2001**, *101*, 1205−1227.
(30) Elliott, G. P.; Roper, W. R.; Waters, J. M. *J. Chem. Soc., Chem. Commun.* **1982**, 811−813.
(31) Xia, H.; He, G.; Zhang, H.; Wen, T. B.; Sung, H. H. Y.; Williams, I. D.; Jia, G. *J. Am. Chem. Soc.* **2004**, *126*, 6862−6863.
(32) Bleeke, J. R.; Behm, R.; Xie, Y.-F.; Chiang, M. Y.; Robinson, K. D.; Beatty, A. M. *Organometallics* **1997**, *16*, 606−623.
(33) Gilbertson, R. D.; Lau, T. L. S.; Lanza, S.; Wu, H.-P.; Weakley, T. J. R.; Haley, M. M. *Organometallics* **2003**, *22*, 3279−3289.
(34) Paneque, M.; Posadas, C. M.; Poveda, M. L.; Rendón, N.; Salazar, V.; Oñate, E.; Mereiter, K. *J. Am. Chem. Soc.* **2003**, *125*, 9898−9899.
(35) Landorf, C. W.; Volker, J.; Weakley, T. J. R.; Haley, M. M. *Organometallics* **2004**, *23*, 1174−1176.
(36) Iron, M. A.; Lucassen, A. C. B.; Cohen, H.; van der Boom, M. E.; Martin, J. M. L. *J. Am. Chem. Soc.* **2004**, *126*, 11699−11710.
(37) Iron, M. A.; Martin, J. M. L.; van der Boom, M. E. *J. Am. Chem. Soc.* **2003**, *125*, 11702−11709.
(38) Iron, M. A.; Martin, J. M. L.; van der Boom, M. E. *J. Am. Chem. Soc.* **2003**, *125*, 13020−13021.
(39) Iron, M. A.; Martin, J. M. L.; van der Boom, M. E. *Chem. Commun.* **2003**, 132−133.
(40) De Proft, F.; Geerlings, P. *Phys. Chem. Chem. Phys.* **2004**, *6*, 242−248.
(41) In molecular orbital theory, the absolute hardness is defined as half the HOMO−LUMO gap.
(42) Camizo, J. A.; Morgado, J.; Sosa, P. *Organometallics* **1993**, *12*, 5005−5007.
(43) Abbotto, A.; Beverina, L.; Bradamante, S.; Facchetti, A.; Klein, C.; Pagani, G. A.; Mesfin, R. A.; Wortmann, R. *Chem.—Eur. J.* **2003**, *9*, 1991−2007.
(44) Chou, S.-S. P.; Hsu, G.-T.; Lin, H.-C. *Tetrahedron Lett.* **1999**, *40*, 2157−2160.
(45) Wong, K. Y.; Jen, A. K.-Y.; Rao, V. P.; Dorst, K. J. *J. Chem. Phys.* **1994**, *100*, 6818−6825.
(46) Rao, V. P.; Jen, A. K.-Y.; Wong, K. Y.; Drost, K. J. *Tetrahedron Lett.* **1993**, *34*, 1747−1750.
(47) Cheng, L.-T.; Tam, W.; Stevenson, S. H.; Meredith, G. R. *J. Phys. Chem.* **1991**, *95*, 10631−10643.
(48) Breitung, E. M.; Shu, C.-F.; McMahon, R. J. *J. Am. Chem. Soc.* **2000**, *122*, 1154−1160.
(49) Albert, I. D. L.; Marks, T. J.; Ratner, M. A. *J. Am. Chem. Soc.* **1997**, *119*, 6575−6582.
(50) Varanasi, P. R.; Jen, A. K. Y.; Chandrasekhar, J.; Namboothiri, I. N. N.; Rathna, A. *J. Am. Chem. Soc.* **1996**, *118*, 12443−12448.
(51) Dirk, C. W.; Katz, H. E.; Schiling, M. L. *Chem. Mater.* **1990**, *2*, 700−705.
(52) Boyd, R. W. *Nonlinear Optics*, 2nd ed.; Academic Press: San Diego, CA, 2003.
(53) Dalton, L. R. *J. Phys.: Condens. Matter* **2003**, *15*, R897−R934.
(54) van der Boom, M. E. *Angew. Chem., Int. Ed.* **2002**, *41*, 3363−3366.
(55) van der Boom, M. E.; Marks, T. J. Layer-by-Layer Assembly of Molecular Materials for Electrooptical Applications. In *Polymers for Microelectronics and Nanoelectronics*; Lin, Q., Ed.; ACS Symposium Series 874; American Chemical Society: Washington, DC, 2004; pp 30−43.
(56) Oudar, J. L. *J. Chem. Phys.* **1977**, *67*, 446−457.
(57) Oudar, J. L.; Chemla, D. S. *J. Chem. Phys.* **1977**, *66*, 2664−2668.
(58) Stiegman, A. E.; Graham, E.; Perry, K. J.; Khundkar, L. R.; Cheng, L.-T.; Perry, J. W. *J. Am. Chem. Soc.* **1991**, *113*, 7658−7666.
(59) Coe, B. J.; Harris, J. A.; Harrington, L. J.; Jeffery, J. C.; Rees, L. H.; Houbrechts, S.; Persoons, A. *Inorg. Chem.* **1998**, *37*, 3391−3399.
(60) Coe, B. J.; Harris, J. A.; Asselberghs, I.; Persoons, A.; Jeffery, J. C.; Rees, L. H.; Gelbrich, T.; Hursthouse, M. B. *J. Chem. Soc., Dalton Trans.* **1999**, 3617−3625.
(61) Albert, I. D. L.; Marks, T. J.; Ratner, M. A. *J. Am. Chem. Soc.* **1998**, *120*, 11174−11181.
(62) Hrobarik, P.; Zahradnik, P.; Fabian, W. M. F. *Phys. Chem. Chem. Phys.* **2004**, *6*, 495−502.
(63) Ray, P. C. *Chem. Phys. Lett.* **2004**, *394*, 354−360.
(64) Mendis, B. A. S.; de Silva, K. M. N. *THEOCHEM* **2004**, *678*, 31−38.
(65) Sitha, S.; Rao, J. L.; Bhanuprakash, K.; Choudary, B. M. *J. Phys. Chem.* **2001**, *105*, 8727−8733.
(66) Liyanage, P. S.; de Silva, R. M.; de Silva, K. M. N. *THEOCHEM* **2003**, *639*, 195−201.
(67) Alparone, A.; Millefiori, A.; Millefiori, S. *Chem. Phys.* **2004**, *298*, 75−86.
(68) Curreli, S.; Deplano, P.; Faulmann, C.; Ienco, A.; Mealli, C.; Mercuri, M. L.; Pilia, L.; Pintus, G.; Serpe, A.; Trogu, F. *Inorg. Chem* **2004**, *43*, 5069−5079.
(69) Romaniello, P.; Lelj, F. *THEOCHEM* **2003**, *636*, 23−37.
(70) Ricciardi, G.; Rosa, A.; van Gisbergen, S. J. A.; Baerends, E. J. *J. Phys. Chem. A* **2000**, *104*, 635−643.
(71) Guerra, C. F.; Snijders, J. G.; te Velde, G.; Baerends, E. J. *Theor. Chem. Acc.* **1998**, *99*, 391−403.
(72) van Gisbergen, S. J. A.; Guerra, C. F.; Baerends, E. J. *J. Comput. Chem.* **2000**, *21*, 1511−1523.
(73) Frisch, M. J.; Trucks, G. W.; Schlegel, H. B.; Scuseria, G. E.; Robb, M. A.; Cheeseman, J. R.; Zakrzewski, V. G.; Montgomery, J. A., Jr.; Stratmann, R. E.; Burant, J. C.; Dapprich, S.; Millam, J. M.; Daniels, A. D.; Kudin, K. N.; Strain, M. C.; Farkas, O.; Tomasi, J.; Barone, V.; Cossi, M.; Cammi, R.; Mennucci, B.; Pomelli, C.; Adamo, C.; Clifford, S.; Ochterski, J.; Petersson, G. A.; Ayala, P. Y.; Cui, Q.; Morokuma, K.; Malick, D. K.; Rabuck, A. D.; Raghavachari, K.; Foresman, J. B.; Cioslowski, J.; Ortiz, J. V.; Stefanov, B. B.; Liu, G.; Liashenko, A.; Piskorz, P.; Komaromi, I.; Gomperts, R.; Martin, R. L.; Fox, D. J.; Keith, T.; Al-Laham, M. A.; Peng, C. Y.; Nanayakkara, A.; Gonzalez, C.; Challacombe, M.; Gill, P. M. W.; Johnson, B. G.; Chen, W.; Wong, M. W.; Andres, J. L.; Head-Gordon, M.; Replogle, E. S.; Pople, J. A. *Gaussian 98*, revision A.11; Gaussian, Inc.: Pittsburgh, PA, 1998.
(74) Frisch, M. J.; Trucks, G. W.; Schlegel, H. B.; Scuseria, G. E.; Robb, M. A.; Cheeseman, J. R.; Montgomery, Jr., J. A.; Vreven, T.; Kudin, K. N.; Burant, J. C.; Millam, J. M.; Iyengar, S. S.; Tomasi, J.; Barone, V.; Mennucci, B.; Cossi, M.; Scalmani, G.; Rega, N.; Petersson, G. A.; Nakatsuji, H.; Hada, M.; Ehara, M.; Toyota, K.; Fukuda, R.; Hasegawa, J.; Ishida, M.; Nakajima, T.; Honda, Y.; Kitao, O.; Nakai, H.; Klene, M.; Li, X.; Knox, J. E.; Hratchian, H. P.; Cross, J. B.; Bakken, V.; Adamo, C.; Jaramillo, J.; Gomperts, R.; Stratmann, R. E.; Yazyev, O.; Austin, A. J.; Cammi, R.; Pomelli, C.; Ochterski, J. W.; Ayala, P. Y.; Morokuma, K.; Voth, G. A.; Salvador, P.; Dannenberg, J. J.; Zakrzewski, V. G.; Dapprich,

S.; Daniels, A. D.; Strain, M. C.; Farkas, O.; Malick, D. K.; Rabuck, A. D.; Raghavachari, K.; Foresman, J. B.; Ortiz, J. V.; Cui, Q.; Baboul, A. G.; Clifford, S.; Cioslowski, J.; Stefanov, B. B.; Liu, G.; Liashenko, A.; Piskorz, P.; Komaromi, I.; Martin, R. L.; Fox, D. J.; Keith, T.; Al-Laham, M. A.; Peng, C. Y.; Nanayakkara, A.; Challacombe, M.; Gill, P. M. W.; Johnson, B.; Chen, W.; Wong, M. W.; Gonzalez, C.; Pople, J. A. *Gaussian 03*, Revision C.01; Gaussian, Inc., Wallingford CT, 2004.

(75) Hamprecht, F. A.; Cohen, A. J.; Tozer, D. J.; Handy, N. C. *J. Chem. Phys.* **1998**, *109*, 6264−6271.

(76) Boese, A. D.; Martin, J. M. L.; Handy, N. C. *J. Chem. Phys.* **2003**, *119*, 3005−3014.

(77) Dolg, M. In *Modern Methods and Algorithms of Quantum Chemistry*; Grotendorst, J., Ed.; John von Neumann Institute for Computing: Jülich, Germany, 2000; Vol. 1, pp 479−508.

(78) van Gisbergen, S. J. A.; Snijders, J. G.; Baerends, E. J. *J. Chem. Phys.* **1998**, *109*, 10644−10656.

(79) van Gisbergen, S. J. A.; Snijders, J. G.; Baerends, E. J. *Comput. Phys. Commun.* **1999**, *118*, 119−138.

(80) te Velde, G.; Bickelhaupt, F. M.; van Gisbergen, S. J. A.; Guerra, C. F.; Baerends, E. J.; Snijders, J. G.; Ziegler, T. *J. Comput. Chem.* **2001**, *22*, 931−967.

(81) Baerends, E. J. ADF 2002.03; Department of Theoretical Chemistry, Free University of Amsterdam, The Netherlands, 2002.

(82) van Lenthe, E.; Baerends, E. J.; Snijders, J. G. *J. Chem. Phys.* **1993**, *99*, 4597−4610.

(83) van Lenthe, E.; Baerends, E. J.; Snijders, J. G. *J. Chem. Phys.* **1994**, *101*, 9783−9792.

(84) van Lenthe, E.; Ehlers, A. E.; Baerends, E. J. *J. Chem. Phys.* **1999**, *110*, 8943−8953.

(85) Schipper, P. R. T.; Gritsenko, O. V.; van Gisbergen, S. J. A.; Baerends, E. J. *J. Chem. Phys.* **2000**, *112*, 1344−1352.

(86) Grüning, M.; Gritsenko, O. V.; van Gisbergen, S. J. A.; Baerends, E. J. *J. Chem. Phys.* **2002**, *116*, 9591−9601.

(87) Lee, A. M.; Colwell, S. M. *J. Chem. Phys.* **1994**, *101*, 9704−9709.

(88) Guan, J.; Duffy, P.; Carter, J. T.; Chong, D. P.; Casida, K. C.; Casida, M. E.; Wrinn, M. *J. Chem. Phys.* **1993**, *98*, 4753−4765.

(89) Dickson, R. M.; Becke, A. D. *J. Phys. Chem.* **1996**, *100*, 16105−16108.

(90) Chong, D. P. *Can. J. Chem.* **1995**, *73*, 79.

(91) March, J. *Advanced Organic Chemistry*, 3rd ed.; John Wiley & Sons: New York, 1985; p 244.

(92) Marder, S. R.; Kippelen, B.; Jen, A. K. Y.; Peyghambarian, N. *Nature (London)* **1997**, *388*, 845−851.

(93) Verbiest, T.; Houbrechts, S.; Kauranen, M.; Clays, K.; Persoons, A. *J. Mater. Chem.* **1997**, *7*, 2175−2189.

(94) Barzoukas, M.; Blanchard-Desce, M.; Josse, D.; Lehn, J.-M.; Zyss, J. *Chem. Phys.* **1989**, *133*, 323−329.

(95) Huijts, R. A.; Hesselink, G. L. J. *Chem. Phys. Lett.* **1989**, *156*, 209−212.

(96) Cheng, L.-T.; Tam, W.; Marder, S. R.; Stiegman, A. E.; Rikken, G.; Spangler, C. W. *J. Am. Chem. Soc.* **1991**, *95*, 10643−10652.

(97) Cheng, L.-T.; Tam, W.; Meredith, G. R.; Marder, S. R. *Mol. Cryst. Liq. Cryst.* **1990**, *189*, 137−153.

(98) Wrighton, M. S.; Morse, D. L. *J. Organomet. Chem.* **1975**, *97*, 405−420.

(99) Cheng, L.-T.; Tam, W.; Eaton, D. F. *Organometallics* **1990**, *9*, 2856−2857.